



XXXI Congresso Nacional de Estudantes de Engenharia Mecânica 29 de Setembro a 03 de Outubro de 2025, São Carlos - SP, Brasil

A comparison between two fatigue damage accumulation rules for composite laminates under multiaxial variable amplitude loading

Samuel Gomes Rodriguez Duran, samuelduran@estudante.ufscar.br¹ Gustavo Fernandes dos Santos, gustavofernandes@id.uff.br² Jorge Alberto Rodriguez Duran, jorgeduran@id.uff.br²

¹Universidade Federal de São Carlos, Rod. Washington Luís, Km 235 – C.P. 676 – 13565-905, São Carlos, São Paulo

Abstract. Composite laminates are widely used in structural elements today and can experience fatigue failures under variable stresses. This paper simulates three stress time series acting at small angles from a multilayer laminate's symmetry system. By breaking down the stress series into groups of constant stress range, mean stress, and frequency, along with material fatigue properties, it predicts the number of cycles to fatigue failure in each group. The cycle ratios can then be accumulated using various methods. The research aims to compare results from two approaches: the Linear Damage Rule (LDR) and the Batsoulas Damage Rule (BDR). Results show that BDR predicts a number of spectra passes much higher than LDR for two of the three stress series, confirming LDR's conservatism.

Keywords: fatigue damage accumulation, variable amplitude loading, rainflow cycle counting, multiaxial stresses, composite laminates

1. INTRODUCTION

Composite materials have been used as structural elements since around 1950, initially as substitutes for traditional ferrous and non-ferrous metals. Despite some similarities in the fatigue process, the fatigue behavior in composites differs significantly from that in metals. Early studies (Owen, 1970) revealed that, due to differences in intrinsic anisotropy and stiffness between fibers and matrix, composite fatigue is governed by several parameters beyond those affecting metals. The key parameters investigated included matrix type, fiber orientation (Salkind, 1972), and mean stress (Boller, 1964).

Numerous experimental programs over the years have improved the understanding of fatigue behavior in composite laminates, resulting in extensive fatigue data, particularly in aerospace and wind energy applications. Public databases like FACT, Optidat, and SNL/MSU/DOE Vallons (2015), Mandell *et al.* (2016) provide valuable data for high cycle fatigue (HCF) assessment through stress versus number of cycles (S-N) equations under both constant amplitude (CA) and variable amplitude (VA) sequences, such as Wisper (Have, 1989) and WisperX (Bulder *et al.*, 2005).

Established fatigue assessment methodologies are based on this characterization of composite laminates. Of particular importance are the results reported by Philippidis et al. (Philippidis and Vassilopoulos, 2002), who conducted an experimental fatigue program on over 250 glass-reinforced plastic coupons in different stress ratios and orientations. This paper uses test results along the fiber direction and at 45° and 90° off-axis. This study focuses on composite structures subjected to high cycle variable amplitude loading. Despite unsolved problems and uncertainties in fatigue-related issues (Schütz, 1996), a standard procedure for fatigue life assessment includes (Philippidis and Vassilopoulos, 2004):

- a) Application of the Rainflow Cycle Counting (RFCC) method.
- b) Superposition of the rainflow pairs on constant life diagrams (CLD).
- Application of the fatigue failure criterion for determining the number of cycles to fatigue failure in each rainflow block.
- d) Use of a damage accumulation rule.

The purpose of the present work is to compare the results of two damage accumulation rules after completing the first three steps. These models include the widely used Linear Damage Rule (LDR) proposed in the 1920s (Palmgren, 1924) and reformulated by Miner in 1945 (Miner, 1945), and the Batsoulas Damage Rule (BDR) (Batsoulas, 2016; Batsoulas and Giannopoulos, 2023), a nonlinear cumulative damage model based on continuum damage mechanics (CDM).

2. THE LINEAR DAMAGE RULE (LDR)

The Linear Damage Rule (LDR), commonly referred to as Miner's rule, is currently the industry standard for designing against fatigue in metallic structures (Hectors and Waele, 2021). This approach calculates an elementary fatigue damage d_i using the cycle ratios n_i/N_{fi} between frequency and fatigue life under specific combinations of the stress amplitude σ_{ai} and the mean stress σ_{mi} contained in the stress signal. For extensive stress histories, it is customary to perform the

²Universidade Federal Fluminense, Av. dos Trabalhadores 420, Santa Cecilia, Volta Redonda 27255-125, Rio de Janeiro

Rainflow Cycle Counting (RFCC) procedure on a signal where turning points have been previously discretized to, for example, u levels (Johannesson, 1999). The results of this counting are typically presented in the u squared rainflow matrix $\mathbf{F} = (n_{ij})_{i,j=1}^u$, containing the frequency n_{ij} of the vectors $\boldsymbol{\sigma_a} = (\sigma_{ai})_{i=1}^u$ and $\boldsymbol{\sigma_m} = (\sigma_{mi})_{i=1}^u$. Since the rainflow matrix comprises u^2 combinations of the triplet $(\sigma_{ai}; \sigma_{mi}; n_i)$, the elementary damage vector is $\mathbf{d} = (d_i)_{i=1}^u$. The total damage according to the LDR is simply the sum of the cycle ratios contained in this vector.

$$D^{LDR} = \sum_{i} d_i = \sum \frac{n_i}{N_{fi}} \tag{1}$$

The critical value for damage is generally considered to be 100% or D=1. The number of fatigue cycles N_{fi} in Eq. 1 can be derived from the S-N equations. These curves, however, depend not only on the stress amplitude but also on the mean stress or, equivalently, on the load ratio $R=\sigma_{min}/\sigma_{max}=(\sigma_a-\sigma_m)/(\sigma_a+\sigma_m)$, as well as on the direction of measurements in the case of anisotropic materials. Composite laminates can be regarded as transversely isotropic materials with their material symmetry system identified by the capital X and Y in the fiber's direction and transverse to them, respectively. Experimental fatigue tests are performed by applying normal stress amplitude at a given load ratio in each of these directions, resulting in the curves $X(N_f,R)$ and $Y(N_f,R)$. Additionally, a shear stress amplitude at a given load ratio provides the S-N curve in the S-direction or $S(N_f,R)$.

If a uniaxial normal stress amplitude σ_{1a} is applied at a given load ratio R in the fiber's direction, for example, the number of fatigue cycles can be readily estimated by equating the fatigue actions (stresses) and the respective material strength in the same direction: $\sigma_{1a} = X(N_f, R)$. Under multiaxial constant amplitude stresses (CA), such as a plane stress state represented by σ_{1a} , σ_{2a} and σ_{6a} (or σ_{ja} (j=1,2,6)) acting on-axis (in the material's symmetry system) with its three components fluctuating in-phase, one approach for computing fatigue life involves the failure tensor polynomial fatigue (FTPF) (Philippidis and Vassilopoulos, 1999):

$$\left(\frac{\sigma_{1a}}{X(N_f, R)}\right)^2 + \left(\frac{\sigma_{2a}}{Y(N_f, R)}\right)^2 - \frac{\sigma_{1a}\sigma_{2a}}{X(N_f, R)Y(N_f, R)} + \left(\frac{\sigma_{6a}}{S(N_f, R)}\right)^2 = 1$$
(2)

It is important to note that in Eq. 2, the capital letters X, Y and S represent strengths, while the subscripts 1, 2 and 6 denote stresses in the respective directions. The N_{fi} term used in the cycle ratios (Eq. 1) is the solution to Eq. 2, provided the strength curves are available at the same load ratio of the fatigue actions.

For variable amplitude (VA) plane stress components, it is still possible to apply a multiaxial RFCC algorithm, such as those proposed in (Wang and Brown, 1996) and (Meggiolaro and de Castro, 2012). A simpler scenario arises if all VA stress histories $\sigma_j(t)$ are parameterized relative to an original, single stress time series. In either case, most of the rainflowed load ratios R_{ji} (j=1,2,6) derived from these stress vectors do not coincide with the load ratios used in the experimental program, meaning the fatigue strength curve under these loads is unknown. For these situations, an interpolation process in constant life diagrams (CLD) (Vassilopoulos *et al.*, 2010b) can be performed to determine a new (non-measured) fatigue strength curve (FSC) at the R_{ji} of interest. Detailed equations for the interpolation process can be found in (Vassilopoulos *et al.*, 2010a).

Miner's rule has faced considerable criticism due to its disregard for load sequence and other factors. Schijve (Schijve, 2009) identifies at least three shortcomings of the rule, especially under VA loading: a) stresses below the fatigue limit can contribute to failure by accelerating crack growth; b) sequences of high to low stresses that induce local yielding, particularly at notches, can lead to fatigue crack retardation and longer fatigue life due to residual stress effects at crack tips; and c) the sensitivity of nascent cracks to fracture depends on their size and load levels. None of these factors are included in Eq. 1. It should also be noted that Schijve's objections pertain to the presence of fatigue cracks, which significantly impact the S-N equations.

3. THE BATSOULAS DAMAGE RULE (BDR)

To address the limitations of the linear damage rule (LDR), several nonlinear approaches were created. Comprehensive reviews on various damage accumulation rules that include both LDR and BDR models were published in 1998 (Fatemi and Yang, 1998) and 2017 (Hectors and Waele, 2021). Many nonlinear damage rules (NLDR) propose raising the cycle ratios d_i to a stress function to account for stress level dependence. Batsoulas and Giannopoulos (Batsoulas and Giannopoulos, 2023) referred to this exponent as $\varphi(\sigma)$, expressed as $d_i^{\varphi(\sigma_i)}$. These authors suggest that the damage process in each material can be associated with a family of S-N curves indicating some degree of fatigue damage. The isodamage strength curves can be mathematically represented by the following hyperbolic expression in normalized coordinates:

$$\left(\log \frac{\sigma}{\sigma_f}\right)^{-1} = C \left(\log \frac{N}{N_m}\right)^{-1} \tag{3}$$

where σ_f and C are fitting constants (material properties), and the parameter N_m is the minimum number of repetitions or fatigue cycles needed for damage initiation. The term N in Eq. 3 can represent $N \equiv N_f$ for $D_f = 1$ (the

conventional S-N curve) or $N \equiv n$ for any non-critical fatigue strength curve. Using geometric arguments, the cycle ratio d_i corresponding to any intermediary (non-critical) isodamage curve can be related to the conventional S-N curve by the following expression:

$$d_{i} = \frac{\left(\log \frac{\sigma}{\sigma_{f}}\right)^{-1} \cdot \log \frac{n}{N_{m}}}{\left(\log \frac{\sigma}{\sigma_{f}}\right)^{-1} \cdot \log \frac{N_{f}}{N_{m}}} \tag{4}$$

which, when extended to multilevel loads and accumulated over the cycles results in:

$$D^{BDR} = \left(\cdots \left(\left(\left(\frac{n_1}{N_{f1}} \right)^{\frac{\log(\sigma_2/\sigma_f)}{\log(\sigma_1/\sigma_f)}} + \frac{n_2}{N_{f2}} \right)^{\frac{\log(\sigma_3/\sigma_f)}{\log(\sigma_2/\sigma_f)}} + \frac{n_3}{N_{f3}} \right)^{\frac{\log(\sigma_4/\sigma_f)}{\log(\sigma_3/\sigma_f)}} + \cdots + \frac{n_{\nu-1}}{N_{f\nu-1}} \right)^{\frac{\log(\sigma_\nu/\sigma_f)}{\log(\sigma_\nu-1/\sigma_f)}} + \frac{n_\nu}{N_{f\nu}} (5)$$

Equation 5 demonstrates that the BDR can incorporate the effects of stress levels on damage calculations. The models utilize only one material property, the fatigue strength coefficient σ_f .

4. METHODOLOGY

We begin this section by recalling the objective of this research: to compare damage life predictions by the LDR and the BDR under multiaxial variable amplitude loading. The four steps mentioned in the introduction for performing a fatigue life assessment task under multiaxial VA loads will be explained here. This section is divided into subsections related to the simulated stress histories (loads), the fatigue properties of the composite laminate, and the comparison between loads and strengths (the fatigue assessment itself). Finally, damage is accumulated according to the two rules.

4.1 Fatigue Actions

To simplify algorithms for RFCC in multiaxial situations, we have parameterized the plane stress components in terms of a single off-axis stress component $\sigma_1^{\theta}(t)$ and its angle θ relative to the on-axis direction (defined as $\theta=0$). To achieve this, the well-known stress transformation equations are used:

$$\sigma_{1}^{0} = \sigma_{1}^{\theta} \cos^{2}(\theta) \qquad \sigma_{2}^{0} = \sigma_{1}^{\theta} \sin^{2}(\theta) \qquad \sigma_{6}^{0} = \sigma_{1}^{\theta} \cos(\theta) \sin(\theta)$$

$$(6)$$

where the on-axis stresses are denoted as σ_j^0 (j=1,2,6). If the independent stress parameter σ_1^θ is scaled to $\sigma_1^\theta/\cos^2(\theta)$, our load simulation can be considered as initially formed by an on-axis uniaxial stress σ_1^0 , which is later applied off-axis forming small angles θ relative to the on-axis direction. This inclined stress induces a multiaxial stress state as described in Eqns. 6. Note that in the same equation, the transverse normal stress σ_2^0 and the shear stress σ_6^0 have a constant relation with σ_1^0 as follows:

$$\sigma_2^0/\sigma_1^0 = \tan^2(\theta) \equiv k^2 \qquad \sigma_6^0/\sigma_1^0 = \tan(\theta) \equiv k \tag{7}$$

Our load simulation consists of three randomly generated stress histories of $\sigma_1^{\theta}(\sigma_m,t)$ with three different mean stresses each $(\sigma_m = [-30,0,30] \, \mathrm{MPa})$ and six angles of misalignment k = [0,.02,.04,.06,.08,.1] resulting in a total of eighteen load scenarios. The first step involves extracting the rainflow matrix F contained in each stress signal. This matrix is essentially a two-dimensional histogram with bins representing the stress ranges (or amplitudes) and mean stresses. Since all other stress components are parameterized relative to $\sigma_1^{\theta}(\sigma_m,t)$, only one RFCC is necessary for each σ_m . For fatigue assessment (i.e., comparison with fatigue strength curves or their alternative representation, the constant life diagrams CLD), only the amplitude bins $\sigma 1ai^{\theta}$ and the ratios $r_{1i} = \sigma_{1ai}^{\theta}/\sigma_{1mi}^{\theta}$ are needed. Both quantities are extracted from F.

4.2 Fatigue Strength

As mentioned earlier, the experimental data utilised in this research are derived from an extensive experimental programme conducted by Philippidis and Vassilopoulos (Philippidis and Vassilopoulos, 2002). The test specimens are composed of a multidirectional E-glass/polyester with a stacking sequence of $[0/(\pm 45)2/0]T$. The ultimate tensile and compressive strengths, UTS and UCS respectively, are detailed in Table 1.

The fatigue strength data are presented in the form of constant life diagrams (CLD) measured along the fiber direction (X), transverse direction (Y), and shear direction (S) (Figure 1). These CLDs plot the fatigue strength data at a locus

Tabela 1. Mean values of the static properties (UTS and UCS) for the E-glass/polyester used in the present work. Data reported in (Philippidis and Vassilopoulos, 2002).

Direction	UTS (MPa)	UCS (MPa)
0^o	245	-217
90°	85	-84
45^o	139	-106

 $S_m \times S_a$ (mean strength x amplitude strength). The lines originating from the centre represent a fixed load ratio $R = S_{max}/S_{min} = (S_m + S_a)/(S_m - S_a)$, and the points on these lines are connected by straight segments indicating the same fatigue life (constant life). For $S_a = 0$, the diagrams converge, both on the tensile and compressive sides, to the static properties shown in Table 1.

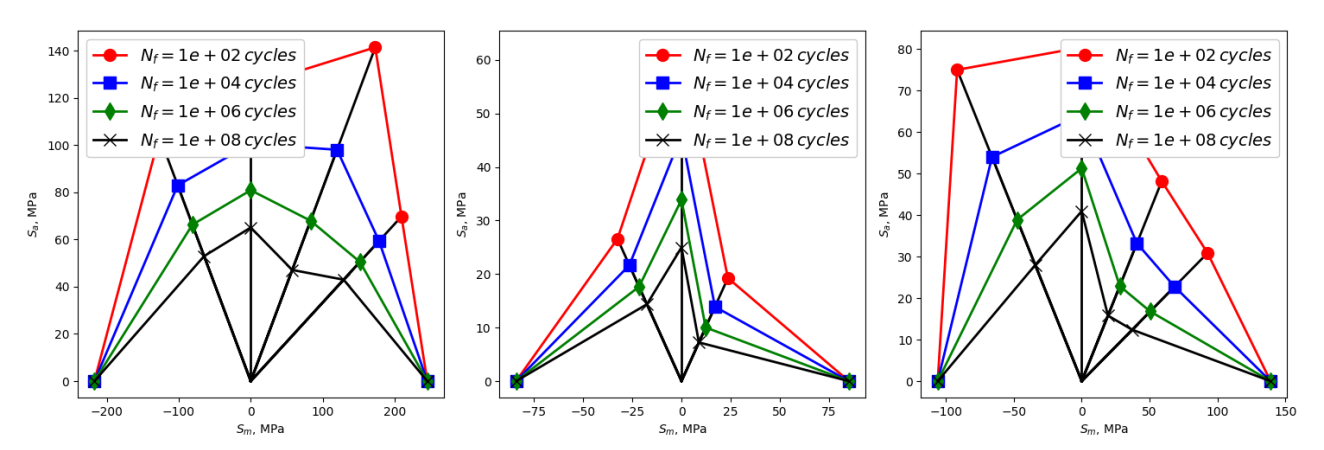


Figura 1. Constant Life Diagrams (CLDs) for the on-axis directions: X, Y, and S, presented from left to right.

4.3 Fatigue Assessment and Damage Accumulation

The load combination composed by σ_{jai} and $R_{ji} = (\sigma_{jmi} + \sigma_{jai})/(\sigma_{jmi} - \sigma_{jai})$ should be used in conjunction with the S-N curve to estimate the fatigue life N_{fi} of the composite laminate. The probability that the load ratio coincides with any of the experimental load ratios (lines departing from the origin in the CLDs) is very low and an interpolation procedure must be developed to estimate the S-N curve corresponding to R_{ji} in each direction. This is schematically depicted in Fig. 2. The load line has a slope $r_{1i} = \sigma_{1ai}^{\theta}/\sigma_{1mi}^{\theta}$ and its intercepts with the lines of constant life provide a set of points $(N_i; S_{ai})$ which can then be fitted by the least square method to obtain the desired S-N curve in the form $S_a = \sigma_f N_f^b$. Both fitting parameters are required to describe the S-N curve, but the fatigue strength coefficient will also be used in Eq. 5.

Two important observations must be made before proceeding: a) do not confuse the load line slope r_{1i} with the load ratio R_{ji} and b) r_{1i} is independent of direction (the subscript j does not apply) due to the parameterization of loads previously explained.

Once the interpolated curves $X(N_f, R_{1i})$, $Y(N_f, R_{2i})$, and $S(N_f, R_{6i})$ are obtained, they are combined with the stress amplitude σ_{jai} in the FTPF criteria (Eq. 2) to solve for N_{fi} . This fatigue life is then combined with the frequency of each load point n_i in the LDR and BDR (Eqns. 1 and 5), resulting in the accumulated fatigue damage D by each rule under the applied load spectra. When D=1, the number of spectra passes is the inverse of the accumulated damage: $N^{LDR}=1/D^{LDR}$ and $N^{BDR}=1/D^{BDR}$.

5. RESULTS AND DISCUSSIONS

The ratio between the predicted spectra for each damage accumulation rule, i.e., $N^{BDR}/N^{LDR} = D^{LDR}/D^{BDR}$, is shown in Fig. 3 for the eighteen load scenarios simulated in this study. Each curve in the figure corresponds to the stress parameter $\sigma_1^{\theta}(\sigma_m,t)$ evaluated at three different mean stress levels σ_m , while the points on these curves represent the variation of the angle parameter, specifically the angle between $\sigma_1^{\theta}(\sigma_m,t)$ and the on-axis direction in the composite laminate.

It is evident from the figure that for stress histories mainly composed of negative values, the predictions based on the BDR are approximately 10% of those based on the LDR. For the other two simulated stress histories, the number of predicted spectra passes by the BDR is significantly greater than the LDR. The angle parameter does not appear to have

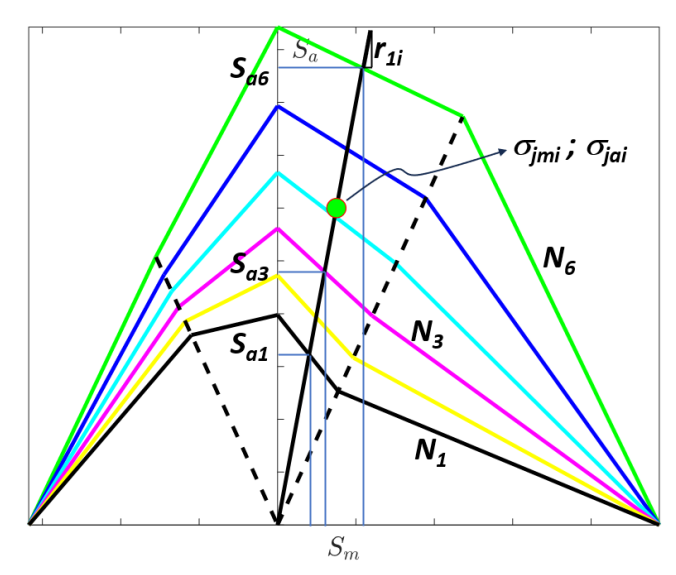


Figura 2. Schematic representation of the interpolation in the CLD looking for S-N curves at a load ratio given by $R_{ji} = (\sigma_{jmi} + \sigma_{jai})/(\sigma_{jmi} - \sigma_{jai}).$

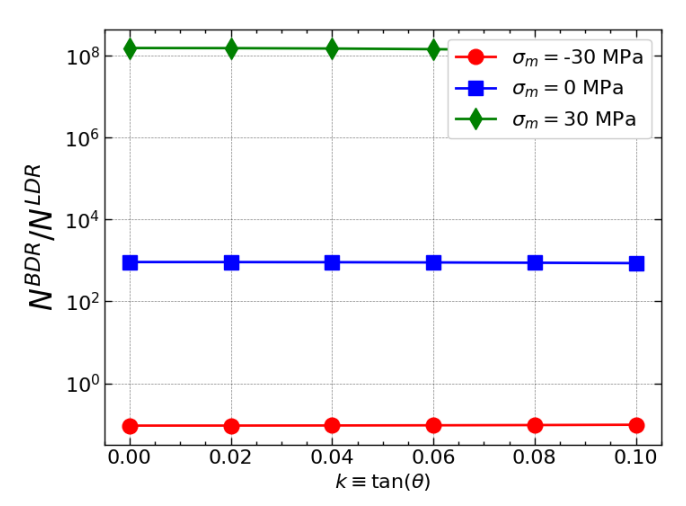


Figura 3. Ratio between the predicted number of spectra passes by the BDR and the LDR for different angles between the applied stress parameter and the material fiber's direction.

an influence; however, the logarithmic scale adopted in the figure, which is necessary for visualizing several orders of magnitude within the same axis system, may obscure any angle effect.

Certain aspects of the damage accumulation process can be effectively illustrated by functions of the type D(d) where $d=\sum_i d_i$ (Fig. 4). This graphical representation helps elucidate several results derived from the current study. The figure depicts four potential trajectories taken by the function D(d). The Linear Damage Rule (LDR) is depicted as a straight line with a slope of one, conforming to Eq. 1 or D(d)=d. Nonlinear damage curves that deviate above or below the linear reference (LDR model) forecast greater or lesser accumulated fatigue damage than Miner's rule, respectively. Given that the simulation under the stress parameter $\sigma_1^\theta(\sigma_m=-30\,\mathrm{MPa},t)$ yields a ratio $N^{BDR}/N^{LDR}\approx 1/10<1$ (Fig. 3), it can be inferred that its D(d) curve (not shown) lies above the LDR model, similar to the $D_{\sigma 3}(d)$ depicted in Fig. 4. In this scenario, the stress signal was primarily characterized by compressive stresses ($\sigma_m=-30\,\mathrm{MPa}$ or compressive-compressive CC loading), and a plausible explanation for the findings could pertain to the generation of tensile residual stresses ahead of potentially propagating cracks, thereby facilitating fatigue crack growth. Evidently, these effects are not accounted for by the LDR model.

Nonlinear damage rules (NLDR) can include stress sequence effects in their predictions, unlike linear damage rules (LDR), where damage is independent of stress order. Nonlinear rules, as shown by the $D_{\sigma_1}(d)$ and $D_{\sigma_2}(d)$ paths in Fig. 4, exceed D=1 for the $\sigma_2 \to \sigma_1$ sequence but not for the inverse sequence. The BDR is a nonlinear approach, demonstrated in Eq. 5. Fatigue life predictions using tensile-compressive (TC) stress series ($\sigma_m=0$ MPa) and tensile-tensile (TT) series ($\sigma_m=30$ MPa) surpass LDR predictions, suggesting BDR curves fall below LDR ones in Fig. 3.

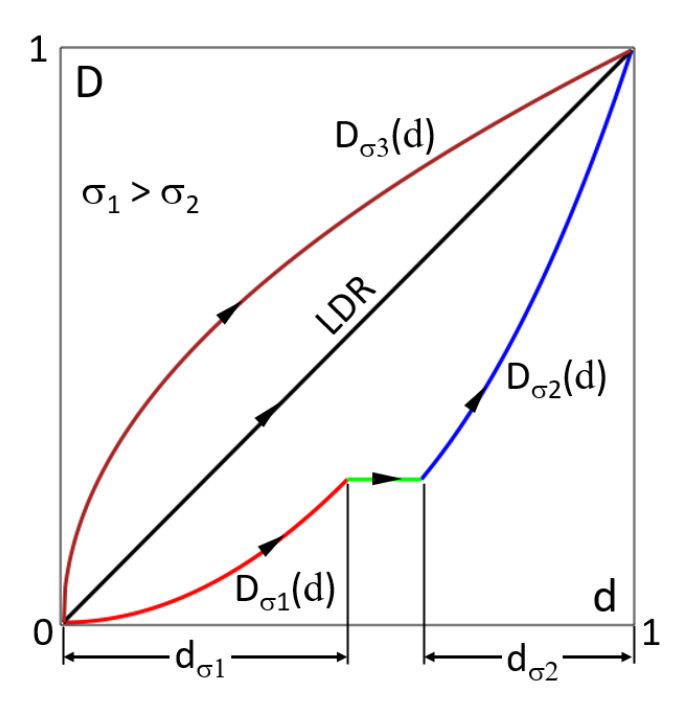


Figura 4. Schematic representation of linear and nonlinear damage rules through the function D(d).

6. CONCLUSIONS

This research compares linear and nonlinear fatigue damage accumulation rules under multiaxial variable amplitude loading across eighteen scenarios. For CC stresses, nonlinear BDR predicted fatigue life at around 10% of the linear LDR. For TC and TT stresses, results were reversed, indicating that Miner's rule is overly conservative in these cases.

7. ACKNOWLEDGMENTS

G. F. dos Santos thanks to *Universidade Federal Fluminense* for the scientific initiation scholarship.

8. REFERENCES

Batsoulas, N.D., 2016. "Cumulative fatigue damage: CDM-based engineering rule and life prediction aspect". *Steel Research International*, Vol. 87, pp. 1670–1677.

Batsoulas, N.D. and Giannopoulos, G.I., 2023. "Cumulative fatigue damage of composite laminates: Engineering rule and life prediction aspect". *Materials*, Vol. 16. ISSN 19961944. doi:10.3390/ma16083271.

Boller, K.H., 1964. "Fatigue characteristics of RP laminates subjected to axial loading". *Modern Plastics*, Vol. 41, No. 10, pp. 145–150.

Bulder, B., Peeringa, J., Lekou, D., Vionis, P., Mouzakis, F., Nijssen, R., Kensche, C., Krause, O., Kramkowski, T., Kauffeld, N. and Söker, H., 2005. "New Wisper - creating a new standard load sequence from modern wind turbine data". Optimat Blades New Wisper - Final Report.

Fatemi, A. and Yang, L., 1998. "Cumulative fatigue damage and life prediction theories: a survey of the state of the art for homogeneous materials". *International Journal of Fatigue*, Vol. 20, pp. 9–34. ISSN 01421123. doi:10.1016/S0142-1123(97)00081-9.

Have, A.t., 1989. "Wisper: introducing variable-amplitude loading in wind turbine design".

Hectors, K. and Waele, W.D., 2021. "Cumulative damage and life prediction models for high-cycle fatigue of metals: A review". *Metals*, Vol. 11, p. 204. ISSN 2075-4701. doi:10.3390/met11020204.

Johannesson, P., 1999. Rainflow Analysis of Switching Markov Loads. Ph.D. thesis, Mathematical Statistics, Center for Mathematical Sciences.

Mandell, J.F., Samborsky, D.D., Miller, D.A., Agastra, P. and Sears, A.T., 2016. "Analysis of SNL/MSU/DOE fatigue database trends for wind turbine blade materials 2010-2015."

Meggiolaro, M.A. and de Castro, J.T.P., 2012. "An improved multiaxial rainflow algorithm for non-proportional stress or strain histories – part II: The modified Wang–Brown method". *International Journal of Fatigue*, Vol. 42, pp. 194–206. ISSN 01421123. doi:10.1016/j.ijfatigue.2011.10.012.

Miner, M., 1945. "Cumulative damage in fatigue". Journal of Applied Mechanics, Vol. 12, pp. A159-A163.

- Owen, M., 1970. "Fatigue testing of fibre reinforced plastics". Composites, Vol. 1, No. 6, pp. 346-355.
- Palmgren, A., 1924. "Life length of roller bearings or durability of ball bearings". Vol. 14, pp. 339-341.
- Philippidis, T.P. and Vassilopoulos, A.P., 1999. "Fatigue strength prediction under multiaxial stress". *Journal of Composite Materials*, Vol. 33, pp. 1578–1599. doi:10.1177/002199839903301701. URL https://doi.org/10.1177/002199839903301701.
- Philippidis, T.P. and Vassilopoulos, A.P., 2002. "Complex stress state effect on fatigue life of GRP laminates. part I, experimental". Technical report.
- Philippidis, T.P. and Vassilopoulos, A.P., 2004. "Life prediction methodology for GFRP laminates under spectrum loading". *Composites Part A: Applied Science and Manufacturing*, Vol. 35, pp. 657–666.
- Salkind, M., 1972. *Fatigue of Composites*, ASTM International100 Barr Harbor Drive, PO Box C700, West Conshohocken, PA 19428-2959, pp. 143–169. doi:10.1520/STP27745S.
- Schijve, J., 2009. Fatigue of Structures and Materials. Springer, 2nd edition.
- Schütz, W., 1996. "A history of fatigue". *Engineering Fracture Mechanics*, Vol. 54, pp. 263–300. ISSN 00137944. doi:10.1016/0013-7944(95)00178-6.
- Vallons, K., 2015. "Databases for fatigue analysis in composite materials". In V. Carvelli and S.V. Lomov, eds., *Fatigue of Textile Composites*, Woodhead Publishing, Woodhead Publishing Series in Composites Science and Engineering, pp. 75–82.
- Vassilopoulos, A.P., Manshadi, B.D. and Keller, T., 2010a. "Influence of the constant life diagram formulation on the fatigue life prediction of composite materials". *International Journal of Fatigue*, Vol. 32, pp. 659–669. ISSN 0142-1123. doi:https://doi.org/10.1016/j.ijfatigue.2009.09.008. URL https://www.sciencedirect.com/science/article/pii/S0142112309002795.
- Vassilopoulos, A.P., Manshadi, B.D. and Keller, T., 2010b. "Piecewise non-linear constant life diagram formulation for FRP composite materials". *International Journal of Fatigue*, Vol. 32, pp. 1731–1738. ISSN 01421123. doi: 10.1016/j.ijfatigue.2010.03.013.
- Wang, C.H. and Brown, M.W., 1996. "Life prediction techniques for variable amplitude multiaxial fatigue—part 1: Theories". *Journal of Engineering Materials and Technology*, Vol. 118, pp. 367–370. ISSN 0094-4289. doi: 10.1115/1.2806821.

9. RESPONSABILITY

The authors are the unique responsible for the information contained in this work.